Design and fabrication of ultrathin silicon-nitride membranes for use in UV-visible airgap-based MEMS optical filters

Mohammadamir Ghaderi and Reinoud F. Wolffenbuttel

Electronic Instrumentation Laboratory, Microelectronics Department, Faculty of EEMCS, Delft University of Technology, Delft, the Netherlands

E-mail: m.ghaderi@tudelft.nl

Abstract. MEMS-based airgap optical filters are composed of quarter-wave thick high-index dielectric membranes that are separated by airgaps. The main challenge in the fabrication of these filters is the intertwined optical and mechanical requirements. The thickness of the layers decreases with design wavelength, which makes the optical performance in the UV more susceptible to fabrication tolerances, such as thickness and composition of the deposited layers, while the ability to sustain a certain level of residual stress by the structural strength becomes more critical. Silicon-nitride has a comparatively high Young's modulus and good optical properties, which makes it a suitable candidate as the membrane material. However, both the mechanical and optical properties in a silicon-nitride film strongly depend on the specifics of the deposition process. A design trade-off is required between the mechanical strength and the index of refraction, by tuning the silicon content in the silicon-nitride film. However, also the benefit of a high index of refraction in a silicon-rich film should be weighed against the increased UV optical absorption. This work presents the design, fabrication, and preliminary characterization of one and three quarter-wave thick silicon-nitride membranes with a one-quarter airgap and designed to give a spectral reflectance at 400 nm. The PECVD silicon-nitride layers were initially characterized, and the data was used for the optical and mechanical design of the airgap filters. A CMOS compatible process based on polysilicon sacrificial layers was used for the fabrication of the membranes. Optical characterization results are presented.

1. Introduction

Optical interference filters based on a stack of alternating layers of two dielectric materials of different index of refraction provide significant potential for system integration of optical MEMS devices, such as microspectrometers and LEDs [1]. The availability of dielectric materials for the fabrication of an optical filter operating in the ultraviolet (UV) and visible range is, however, limited by several constraints. The most important limitation is the presence of absorption peaks of many common dielectric materials in the UV. CMOS process compatibility requirements further limit the list of materials that can be used for the fabrication of an optical filter. Using airgap-based interference filters provide a MEMS-compatible solution for the fabrication of high-performance optical filters in a CMOS-compatible fashion. Although UV and visible airgap-based optical filters using III-V materials have been investigated for LEDs [1], the silicon-based UV and visible MEMS airgap filters have only recently received attention [2].

The main challenge in the fabrication of airgap optical filters is maintaining optical flatness over the freestanding membrane [3]. Therefore, a tensile stressed membrane is required, while the stress gradient in the film has to be sufficiently low [3]. Filters composed of one or several layers with a thickness in the order of one Quarter-Wave Optical Thickness at the design wavelength (1 QWOT) have been considered, but it is extremely difficult to achieve a sufficient level of tensile stress without a stress gradient in such a thin layer (i.e. $\lambda_o/4n$, where n is the refractive index of the material; 70 nm for $\lambda_o = 400$ nm and $n \approx 1.5$) for a taut membrane without rupturing. Straining methods have been investigated to obtain optical flatness in silicon-oxide membranes, however, only a limited improvement was achieved [4].

An alternative approach is to use high Young's modulus materials, such as polysilicon and silicon-nitride, for the membrane material. Furthermore, the filters are composed of several layers with thicknesses in the order of multiples of the quarter-wavelength. The interference condition in the filters is generally satisfied by using (odd n) higher order designs (n-QWOT), thus thicker membranes could be considered, which would result in a similar spectral response.

The fabrication process and the preliminary results of ultrathin silicon-nitride membranes for airgap optical filter application have been investigated. Silicon-nitride thin-films were deposited using PECVD and subsequently annealed to obtain tensile stress. The residual stress and optical properties of the deposited thin films were characterized, and the results are presented in this paper. One-period ($N = 1$) airgap optical filters operating at 400 nm based on 1 QWOT and 3 QWOT silicon-nitride membrane were designed. The fabrication was carried out based on a CMOS-compatible fabrication process followed by a stiction-free drying process. Finally, the fabricated samples were optically characterized, and the results are discussed.

2. PECVD silicon-nitride as the membrane material in airgap optical filters

The excellent mechanical properties of silicon-nitride made it a suitable candidate for use in most MEMS devices. The Young's modulus of Silicon-nitride is about 200 GPa for the films deposited using PECVD [5]. This Young's modulus is significantly higher than the reported value for silicon-oxide (70 GPa [6]). The deformation energy and force in a membrane is inversely proportional to the Young's modulus of the film. Therefore, using silicon-nitride results in a decrease in membrane deformation, hence improving the flatness of the released membrane. In addition, the PECVD deposition of silicon-nitride films provides several advantages, such as the ability to tune the residual stress and optical properties of the deposited films. Therefore, the residual stress of the silicon-nitride can be tuned to obtain tensile stress films [5]. Finally, the etch rate of silicon-nitride in TMAH is very low [7], thus, can be used as a membrane material in combination with polysilicon sacrificial layers.

Table 1. Deposition parameters of PECVD silicon-nitride

SiH_4	0.28 slm
NH_3	1.8 slm
N_2	1 slm
HF/LF power	0.32/0.48 kW
Substrate Temperature	400 °C
Total pressure	2.8 Torr

In this research, the silicon-nitride films were deposited using PECVD and the deposition parameters are listed in Table 1. While the as-deposited residual stress of silicon-nitride films was measured to be equal to -200 MPa (compressive), the residual stress was increased to about 1 GPa (tensile) after an annealing cycle at $600°C$. This high tensile residual stress further ensures the flatness in the released membranes.

3. Optical design

3.1. Optical characterization of silicon-nitride

The optical properties of silicon nitride layers have been extensively studied (e.g. [8, 9]). In PECVD silicon-nitride layers, the gas phase composition of the plasma affects the silicon-to-nitrogen (Si/N) ratio in the films. As a result, the refractive index of the films varies linearly from 1.9 to 2.6 with an increasing Si content of the film (Si/N ratio from 0.7 to 1.7) [9]. Therefore, films with high refractive index can be deposited. The quality of the material combination used in a filter design is usually expressed in terms of their refractive index contrast. Therefore, silicon-rich nitride is in principle highly suitable for optical applications. However, the increased absorption of silicon-rich nitride is a limiting factor in optical applications. Increasing the silicon content in the deposited films results in a spectral shift of the absorption peak in the film toward the longer wavelengths. For instance, the absorption coefficient becomes significant (is higher than $\alpha = 10^3 cm^{-1}$) for stoichiometric Si_3N_4 for wavelengths shorter than about 270 nm ($k = 0.002$), while this limit increases to 800 nm ($k = 0.006$) for silicon-rich Si_9N_4 [8]. Therefore, the trade-off between the refractive index and absorption coefficient must be considered when designing a nitride-based interference optical filter.

The refractive index and extinction coefficient of the deposited nitride layer were measured using ellipsometry. Figure 1 shows the refractive index and absorption coefficient of the films. Although the extinction coefficient of the deposited silicon-nitride at 400 nm is significant ($k = 0.06$), the nitride-based designs are still highly interesting. This stems from the higher refractive index of silicon-nitride, as compared to the silicon-oxide, while the loss in one QWOT layers remains limited to $1 - exp(-\alpha d) = 0.08$. The refractive index contrast ($(n_H^2 - n_L^2)/2n_H^2$; a unitless quality factor between 0 and 0.5) is an important criterion for assessment of the thin films for the optical applications. The higher refractive index of nitride results in a considerable increase in the refractive index contrast (i.e. 43% increase in refractive index contrast as compared to the silicon-oxide with air pair). Furthermore, due to the high refractive index of silicon nitride, a QWOT of silicon-nitride is thinner, thus, the intensity loss due to the absorption is smaller.

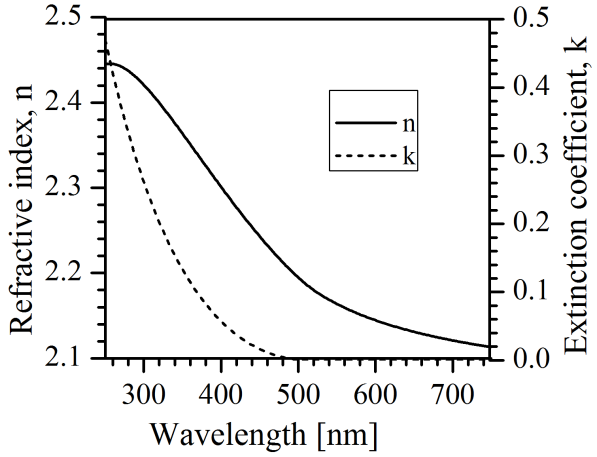

Figure 1. The refractive index and extinction coefficient of PECVD silicon nitride thin-films measured by Ellipsometry.

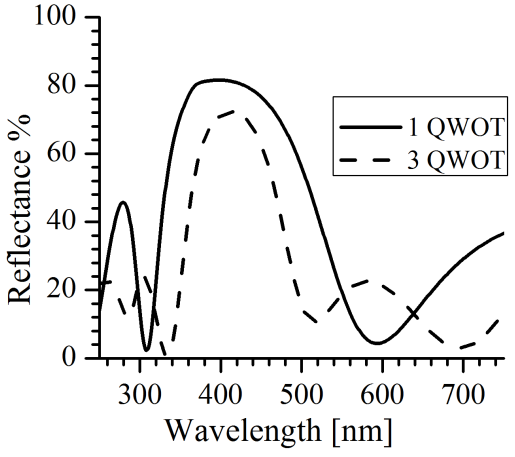

Figure 2. Expected reflectance of a single period ($N = 1$) DBR with 1 QWOT and 3 QWOT membrane simulated using transfer matrix method. The model is based on a silicon (substrate)/silicon-oxide (passivation)/airgap/silicon-nitride structure.

3.2. Optical design of a distributed Bragg grating

A distributed Bragg reflector (DBR) is one of the simplest forms of an optical filter and is composed of a repetitive and alternating high and low index quarter-wave thick layers. In general, any layer with a thickness equal to the odd-multiple of the quarter-wave also satisfies the interference condition and results in a similar spectral reflectance. In this research single period ($N = 1$) DBRs with single-quarter (1 QWOT) and three-quarter-wave thick (3 QWOT) layers, have been designed. Figure 2 shows the expected reflectance of the DBRs simulated using transfer matrix method (TFCalc).

As shown in Figure 2, a 1 QWOT membrane separated by a 1 QWOT airgap result in a peak reflectance of about 82% with a bandwidth of 192 *nm*. The 3 QWOT membrane separated by 1 QWOT airgap design, on the other hand, results in a peak reflectance of 72% and bandwidth of 121 *nm*. The reduced peak reflectance in the 3 QWOT design is due to the increase in the spectral absorption in the thicker membrane layer. Therefore, the 3 QWOT membranes are not very suitable for optical designs, especially when multiple periods of high and low index layers are required.

4. Fabrication

A CMOS-compatible process for fabrication of free-standing silicon-oxide membranes using polysilicon sacrificial layers was already introduced by our group [2, 10]. A similar fabrication process was used for the fabrication of silicon-nitride membranes. The fabrication was performed on prime 10 cm diameter silicon wafers. Figure 3 shows the schematic of the fabrication process. A repetitive deposition of LPCVD polysilicon and PECVD silicon-nitride was performed to build the layer stack according to the optical design. Polysilicon layers are used as the sacrificial layers, thus the thickness was chosen equal to the thickness of the airgap layers. After the deposition of the layer stack, a set of openings was patterned and etched through the deposited layers. An additional silicon nitride layer was deposited using PECVD to cover the openings. The reminder of this layer is then removed, leaving pin-shaped structures for anchoring the membranes after the release. A final patterning and etching of windows provide access for the sacrificial etching. Finally, wet etching in a TMAH-based solution followed by a stiction-free drying using CO_2 at its critical point was used to release the structures.

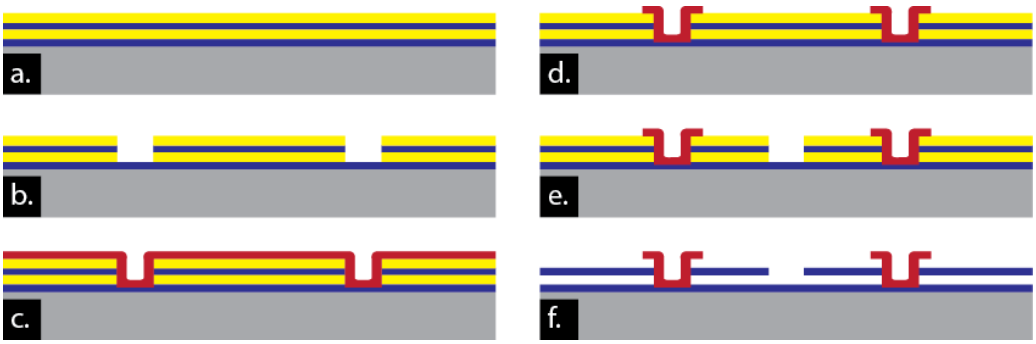

Figure 3. Schematics of the fabrication process.

5. Characterization

Several samples were partially under-etched and went through the critical point drying process. The etching was stopped before the complete removal of the sacrificial material to find out the maximum achievable membrane size, while maintaining a high yield. Figure 4a and 5a show the microscope images of the released samples. The fabricated 1 QWOT and 3 QWOT membranes

have a diameter-to-thickness ratio of about 500 and 150 respectively. Figure 4b and 5b show the show the 45° tilted SEM images of the partially released membranes.

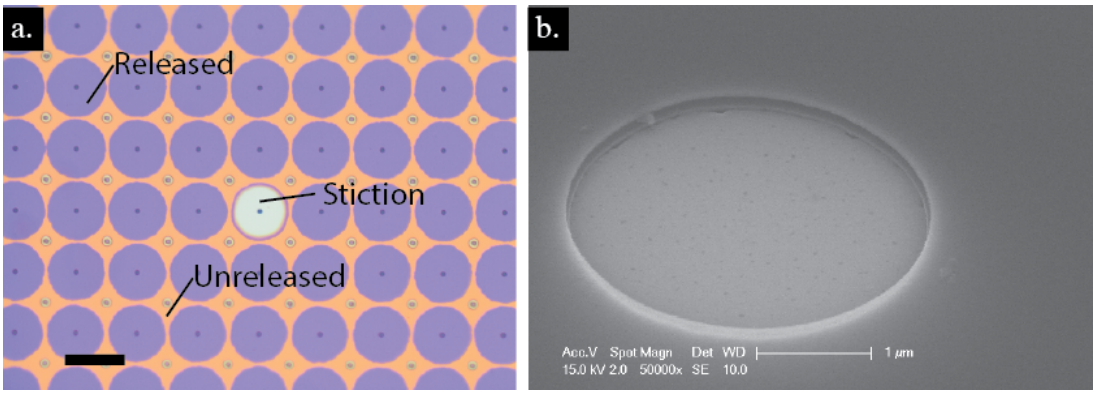

Figure 4. The 1 QWOT silicon nitride membrane separated by a 1 QWOT airgap: a) microscope image, the scale shown in the figure is 25 μm; b) 45° degree tilted SEM micrograph of a circular opening used for the sacrificial etching.

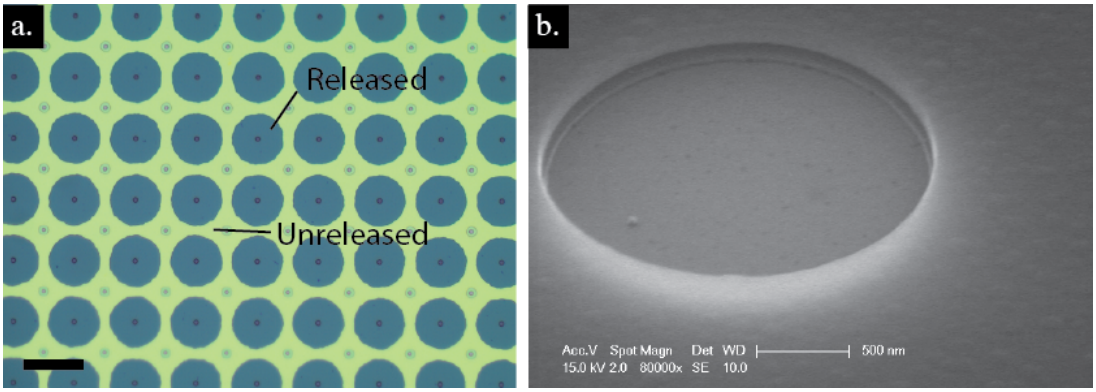

Figure 5. The 3 QWOT silicon nitride membrane separated by a 1 QWOT airgap: a) microscope image, the scale shown in the figure is 25 μm; b) 45° degree tilted SEM micrograph of a circular opening used for the sacrificial etching.

The spectral reflectance of the released samples was measured using a reflection probe with a core diameter of 200 μm. The input fibre channel was coupled to a white light source, and the output was fed to a spectrometer module (Flame, Ocean optics). The samples were placed about $1-2$ mm far from the fibre probe tip. Figures 6 a and b show the spectral reflectance of samples with a 1 QWOT and 3 QWOT silicon-nitride membrane over an area of about $2-3$ mm^2. Due to the large inspection area, several 100-s of filter elements are simultaneously illuminated, and the measured spectral reflectance is a combination of the spectral response from the released and the unreleased areas, while the posts and access holes are accounted for in the device area fill factor. The spectral reflectance reveals a peak at 400 nm, which is associated with the released membranes (about 90% fill factor), is present in Figure 6. Furthermore, the peak at longer wavelengths (about 600 nm) is due to the part of the area with the unreleased structures and is an indication of fabrication yield. An increase in the released area results in an increasing peak at 400 nm, while the peak at 600 nm decreases.

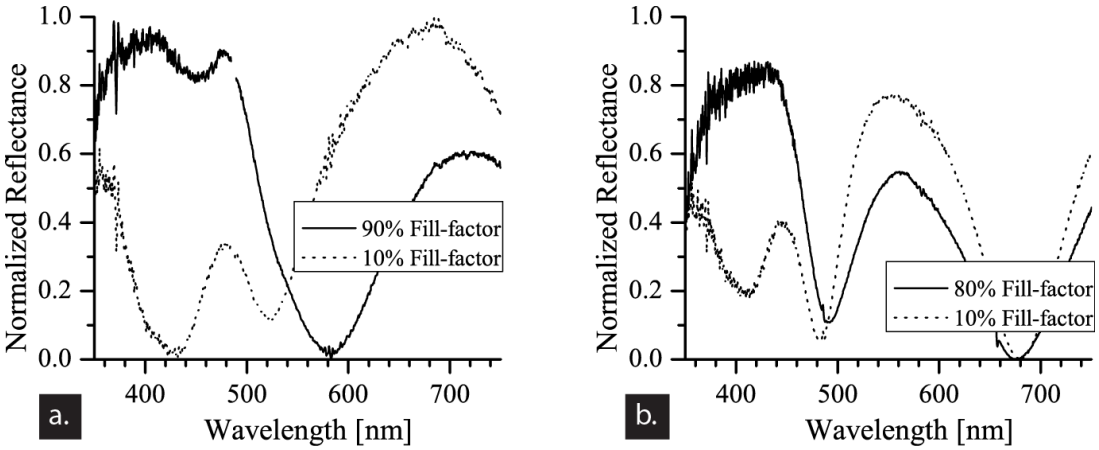

Figure 6. The large area spectral reflectance of a) the 1 QWOT membrane design and b) the 3 QWOT design.

6. Conclusion

In this paper, we present the design, fabrication, and preliminary results on several 1 QWOT and 3 QWOT membranes. Silicon-nitride is a suitable candidate for the large area free-standing membranes. Although silicon-nitride has many advantages, such as the high Young's modulus, ability to obtain a tensile stress, and high refractive index, the main disadvantage is its high extinction coefficient in the UV spectral range. Silicon-nitride films were deposited using PECVD and the mechanical and optical characteristics of the films were measured. A tensile stress of 1 GPa was achieved through annealing of the layer. Although the absorption coefficient in the deposited layers cannot be disregarded, a good spectral response can be achieved due to the high refractive index of the layers. The measured spectral reflection was also in good agreement with the expected response. On-going work is directed towards the fabrication advanced optical filters with higher periods ($N > 1$) and compound silicon-nitride/silicon-oxide membranes.

Acknowledgment

This work has been supported by the Dutch Technology Foundation STW under Grant DEL.11476. The process was carried out in the Else Kooi Laboratory (DIMES) and the Kavli nanolab both at Delft University of Technology.

References

[1] Chen D and Han J 2012 *Applied Physics Letters* **101** 221104
[2] Ghaderi M, Ayerden N P, de Graaf G and Wolffenbuttel R F 2014 *Procedia Engineering* **87** 1533 – 1536
[3] Ghaderi M, Karimi Shahmarvandi E, de Graaf G and Wolffenbuttel R F 2016 *Proc. Conf. on Micro-Optics* vol 9889 (SPIE) pp 98890A–98890A–9
[4] Ghaderi M, de Graaf G and Wolffenbuttel R F 2016 *Proc. Conf. on Micro-Optics* vol 9888 (SPIE) pp 98880R–98880R–8
[5] Zorman C A, Roberts R C and Chen L 2011 *MEMS Materials and Processes Handbook* (Boston, MA: Springer US) ISBN 978-0-387-47318-5
[6] Thurn J and Cook R F 2002 *Journal of Applied Physics* **91** 1988–1992
[7] Paranjape M, Pandy A, Brida S, Landsberger L, Kahrizi M and Zen M 2000 *Journal of Vacuum Science & Technology A* **18** 738–742
[8] Philipp H R 1973 *Journal of The Electrochemical Society* **120** 295–300
[9] Claassen W A P, Valkenburg W G J N, Habraken F H P M and Tamminga Y 1983 *Journal of The Electrochemical Society* **130** 2419–2423
[10] Ghaderi M, Ayerden N P, de Graaf G and Wolffenbuttel R F 2015 *Proc. Conf. on Micro-Optics* vol 9517 (SPIE) pp 95171M–95171M–6